First Observation of $D^0 - \bar{D}^0$ Oscillations in $D^0 \to K^+\pi^-\pi^+\pi^-$ Decays and Measurement of the Associated Coherence Parameters

R. Aaij *et al.*[*]

(LHCb Collaboration)

Charm meson oscillations are observed in a time-dependent analysis of the ratio of $D^0 \to K^+\pi^-\pi^+\pi^-$ to $D^0 \to K^-\pi^+\pi^-\pi^+$ decay rates, using data corresponding to an integrated luminosity of 3.0 fb^{-1} recorded by the LHCb experiment. The measurements presented are sensitive to the phase-space averaged ratio of doubly Cabibbo-suppressed to Cabibbo-favored amplitudes $r_D^{K3\pi}$ and the product of the coherence factor $R_D^{K3\pi}$ and a charm mixing parameter $y'_{K3\pi}$. The constraints measured are $r_D^{K3\pi} = (5.67 \pm 0.12) \times 10^{-2}$, which is the most precise determination to date, and $R_D^{K3\pi} y'_{K3\pi} = (0.3 \pm 1.8) \times 10^{-3}$, which provides useful input for determinations of the CP-violating phase γ in $B^\pm \to DK^\pm$, $D \to K^\mp\pi^\pm\pi^\mp\pi^\pm$ decays. The analysis also gives the most precise measurement of the $D^0 \to K^+\pi^-\pi^+\pi^-$ branching fraction, and the first observation of D^0–$\bar{D}^0$ oscillations in this decay mode, with a significance of 8.2 standard deviations.

Neutral mesons can oscillate between their particle and antiparticle states. This phenomenon, also referred to as mixing, is of considerable interest for a variety of reasons, including its unique sensitivity to effects beyond the standard model of particle physics. Mixing has been observed in strange, beauty, and, most recently, charm mesons. Its observation in the charm ($D^0 - \bar{D}^0$) system is particularly challenging, with an oscillation period that is more than 1000 times longer than the meson's lifetime. It took until 2008 for charm mixing to be established, by combining results from *BABAR*, BELLE, and CDF [1–4], and until 2013 for the first 5σ observation in an individual measurement [5]. Until now, all 5σ observations of charm mixing in individual measurements have been made in the decay mode $D^0 \to K^+\pi^-$ [5–7]. (Unless otherwise stated, the inclusion of charge-conjugate modes is implied throughout.) This Letter reports the first observation of charm mixing in a different decay channel, $D^0 \to K^+\pi^-\pi^+\pi^-$. Previous studies of this decay mode have been consistent with the no-mixing hypothesis [8,9]. Charm mixing is also sensitive to the phase difference between charm and anticharm decay amplitudes to the same final state. This phase information plays an important role in the measurement of the charge-parity (CP) violating phase γ (or ϕ_3), which is accessible in decays with $b \to u$ quark transitions. The precision measurement of the relative magnitudes and phases of quark transitions

provides a stringent test of the standard model, and the parameter γ plays a central role in this effort. Currently, γ has a relatively large experimental uncertainty, and can be measured, with negligible uncertainty from theory input, in the decay $B^+ \to DK^+$ (and others), where D represents a superposition of D^0 and $\bar{D}^0$ states [10–14]. In order to constrain γ using these decay modes, external input is required to describe both the interference and relative magnitude of $D^0 \to f$ and $\bar{D}^0 \to f$ amplitudes, where f represents the final state of the D decay. Previously, it was thought that the relevant phase information could only be measured at e^+e^- colliders operating at the charm threshold, where correlated $D\bar{D}$ pairs provide well-defined superpositions of D^0 and $\bar{D}^0$ states. Recent studies [15,16] have shown that this input can also be obtained from a time-dependent measurement of D^0–$\bar{D}^0$ oscillations. This is the approach followed here.

In this work the observation of D^0–$\bar{D}^0$ oscillations is made by measuring the time-dependent ratio of $D^0 \to K^+\pi^-\pi^+\pi^-$ to $D^0 \to K^-\pi^+\pi^-\pi^+$ decay rates. The flavor of the D meson at production is determined using the decays $D^*(2010)^+ \to D^0\pi_s^+$ and $D^*(2010)^- \to \bar{D}^0\pi_s^-$, where the charge of the soft (low-momentum) pion π_s tags the flavor of the meson. The wrong-sign (WS) decay $D^0 \to K^+\pi^-\pi^+\pi^-$ has two dominant contributions: a doubly Cabibbo-suppressed (DCS) amplitude, and a D^0–$\bar{D}^0$ oscillation followed by a Cabibbo-favored (CF) amplitude. The right-sign (RS) decay $D^0 \to K^-\pi^+\pi^-\pi^+$ is dominated by the CF amplitude, and has negligible contributions of $\mathcal{O}(10^{-4})$ from D^0–$\bar{D}^0$ oscillations. Ignoring CP violation, to second order in t/τ, the time dependence of the phase-space integrated decay rate ratio $R(t)$ is approximated by

$$R(t) = \frac{\Gamma[D^0 \to K^+\pi^-\pi^+\pi^-](t)}{\Gamma[D^0 \to K^-\pi^+\pi^-\pi^+](t)}$$

$$\approx (r_D^{K3\pi})^2 - r_D^{K3\pi} R_D^{K3\pi} y'_{K3\pi} \frac{t}{\tau} + \frac{x^2+y^2}{4}\left(\frac{t}{\tau}\right)^2, \quad (1)$$

where Γ denotes the decay rate, t is the proper decay time of the D^0 meson (measured with respect to production), τ is the D^0 lifetime, and $r_D^{K3\pi}$ gives the phase space averaged ratio of DCS to CF amplitudes [15,16]. The dimensionless parameters x and y describe mixing in the D^0 meson system, with x proportional to the mass difference of the two mass eigenstates, and y proportional to the width difference [4]. Here, $y'_{K3\pi}$ is defined by $y'_{K3\pi} \equiv y \cos\delta_D^{K3\pi} - x \sin\delta_D^{K3\pi}$, where $\delta_D^{K3\pi}$ is the average strong phase difference; this and the coherence factor $R_D^{K3\pi}$ are defined by $R_D^{K3\pi} e^{-i\delta_D^{K3\pi}} \equiv \langle\cos\delta\rangle + i\langle\sin\delta\rangle$, where $\langle\cos\delta\rangle$ and $\langle\sin\delta\rangle$ are the cosine and sine of the phase of the ratio of the DCS to the CF amplitude, averaged over phase space. [The convention $CP|D^0\rangle = +|\bar{D}^0\rangle$ is followed, which determines the sign of the linear term in Eq. (1)]. For the range of D^0 decay times used in this analysis, $[0.5, 12.0] \times \tau$, Eq. (1) is correct to within $\mathcal{O}(10^{-6})$. All three parameters, $r_D^{K3\pi}$, $R_D^{K3\pi}$, and $\delta_D^{K3\pi}$, are required to determine γ in $B^+ \to DK^+$, $D \to K^-\pi^+\pi^-\pi^+$ decays.

This analysis is based on data samples collected in 2011 and 2012 with the LHCb detector at center-of-mass collision energies of $\sqrt{s} = 7$ and 8 TeV corresponding to integrated luminosities of 1.0 and 2.0 fb^{-1}, respectively. The LHCb detector [17,18] is a single-arm forward spectrometer covering the pseudorapidity range $2 < \eta < 5$, designed for the study of particles containing b or c quarks. The detector elements that are particularly relevant to this analysis are a silicon-strip vertex detector surrounding the pp interaction region that allows c and b hadrons to be identified from their characteristically long flight distance, a tracking system that provides a measurement of the momentum p of the charged particles, and two ring-imaging Cherenkov detectors that are able to discriminate between different species of charged hadrons. Simulated events are produced using the software described in Refs. [19–22]. Differences between data and simulation are corrected using data-driven techniques described in Refs. [23,24].

Events are first selected by the LHCb trigger [25], and then by additional off-line requirements. Four tracks in the event must be consistent with the decay $D^0 \to K^+\pi^-\pi^+\pi^-$, each with momentum $p > 3$ GeV/c and transverse momentum $p_T > 350$ MeV/c. The D^0 daughters are required to be inconsistent with originating from a primary pp interaction vertex (PV) and are combined to form a D^0 candidate, which must have a good vertex quality and $p_T > 4.7$ GeV/c. The soft pion, which is combined with the D^0 candidate to form a D^{*+} candidate, is required to satisfy $p > 3$ GeV/c and $p_T > 360$ MeV/c. The D^{*+} candidate must have a good vertex quality, and is reconstructed under the constraint that it originates from its associated PV. In order to suppress backgrounds where tracks are misidentified or misreconstructed, information from the particle identification and tracking systems is used. Secondary decays, i.e., D^{*+} mesons from the decay of a b hadron, are rejected by requiring that the D^0 meson candidate is consistent with originating from a PV. Only D^0 candidates that are reconstructed within 24 MeV/c^2 of the D^0 meson mass [26] are used in the analysis, reducing the amount of partially reconstructed and misidentified background. To reduce combinatorial background from randomly associated soft pions there is also a requirement that the invariant mass difference $\Delta m \equiv m(K^+\pi^-\pi^+\pi^-\pi_s^\pm) - m(K^+\pi^-\pi^+\pi^-)$ is less than 155 MeV/c^2. Approximately 4% of events that pass the selection requirements contain multiple signal candidates. In such cases one candidate is picked at random and the rest are discarded.

Figure 1 shows the Δm distribution of WS and RS signal candidates with the results of a binned likelihood fit
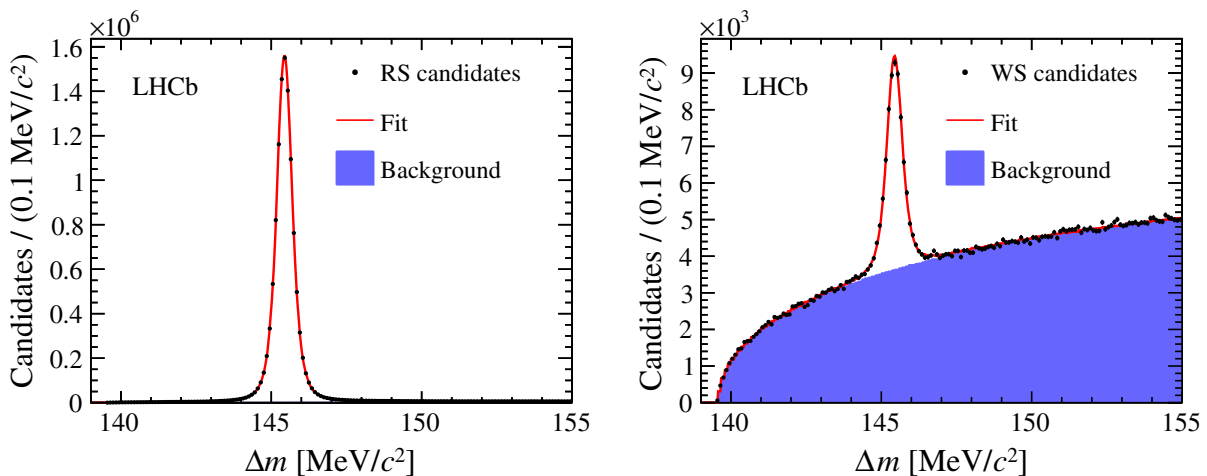

FIG. 1.   Decay-time integrated Δm distributions for RS (left) and WS (right) candidates with the fit result superimposed.

superimposed. The fit includes both a signal and a combinatorial background component: the signal component is empirically described by the sum of a Johnson function [27] and three Gaussian functions. The background component is estimated by randomly associating D^0 candidates with soft pions from different events. The resulting shape is multiplied by a first-order polynomial whose parameters are free to vary in the fit. The fit is made simultaneously to four decay categories: WS and RS modes for D^0 and $\bar{D}^0$ mesons. The background parametrization is free to vary independently in each category, whereas the signal shape is shared between WS and RS categories for each D^{*+} flavor. The RS (WS) yield estimated from the fit corresponds to 11.4×10^6 (42 500) events.

To study the time dependence of the WS/RS ratio, the Δm fitting procedure is repeated in ten independent D^0 decay-time bins. Parameters are allowed to differ between bins. The WS/RS ratio in each bin is calculated from $\sqrt{(N_{\mathrm{WS}D^0} N_{\mathrm{WS}\bar{D}^0})/(N_{\mathrm{RS}D^0} N_{\mathrm{RS}\bar{D}^0})}$, where N denotes the signal yield estimated from the fit for each of the four decay categories. Using the double ratio ensures that any D^{*+}/D^{*-} production asymmetries or differences in π_s^+/π_s^- detection efficiency largely cancel.

Several sources of systematic effects are considered that could bias the measured WS/RS ratio. Candidates in which both a kaon and an oppositely charged pion are misidentified have a very broad structure in $m(K^+\pi^-\pi^+\pi^-)$, but a signal-like shape in Δm. This background artificially increases the measured WS/RS ratio by causing RS decays to be reconstructed as WS candidates. In each decay-time bin i the number of misidentified decays $N_{\mathrm{ID},i}$ is estimated from WS candidates that are reconstructed further than $40 \text{ MeV}/c^2$ from the D^0 mass [26]. The additive correction to the WS/RS ratio is calculated as $\Delta_{\mathrm{ID},i} = N_{\mathrm{ID},i}/N_{\mathrm{RS},i}$, where $N_{\mathrm{RS},i}$ is the number of RS decays in the same decay-time bin. In the entire WS sample it is estimated that 2334 ± 65 misidentified decays are present, constituting $\sim 5.5\%$ of the measured WS signal yield.

The decay $D^0 \to K^+\pi^-K^0_S$, $K^0_S \to \pi^+\pi^-$ has the same final state as signal decays, but a small selection efficiency due to the long flight distance of the K^0_S. Unlike signal decays, the RS and WS categories of this decay have comparable branching fractions [26]. Assuming that the fraction of $D^0 \to K^-\pi^+K^0_S$ decays in the RS sample is negligible, the additive correction to the WS/RS ratio is calculated as $\Delta_{K^0_S} = N_{K^0_S}/N_{RS}$, where $N_{K^0_S}$ is the number of $D^0 \to K^+\pi^-K^0_S$ decays in the WS sample. From a fit to both combinations of $m(\pi^+\pi^-)$, an estimate of $N_{K^0_S} = 590 \pm 100$ is obtained, constituting $\sim 1.4\%$ of the measured WS signal yield. This background is observed to have the same decay-time dependence as RS candidates; therefore, the same correction of $\Delta_{K^0_S} = (6.1 \pm 1.0) \times 10^{-5}$ is applied to the WS/RS ratio in each decay-time bin.

Another background is due to a small fraction of soft pions that are reconstructed with the wrong charge

assignment. Such candidates are vetoed by strict requirements on the track quality. Possible residual background of this type is accounted for by assigning a systematic uncertainty of 2.7×10^{-5} to the measured WS/RS ratio in each decay-time bin.

The systematic uncertainties assigned for $D^0 \to K^+\pi^-K^0_S$ decays and misreconstructed soft pions are both expected to be highly correlated between decay-time bins. Therefore, a correlation coefficient of 1.0 is used between every pair of decay-time bins, which is confirmed as the most conservative approach.

Additional systematic uncertainties are also included for partially reconstructed decays, which are estimated to make up $\sim 0.25\%$ of the measured WS yield, and the choice of signal and background parametrizations used to determine the signal yields. The effect of bin migration due to decay-time resolution has been shown to be negligible [5,28].

Contributions from secondary decays can bias the measured WS/RS ratio because the D^0 decay time is measured with respect to the PV, which for secondary decays does not coincide with the D^0 production vertex; this causes the D^0 decay time to be overestimated. The expected WS/RS ratio in bin i can be written as $\tilde{R}_i[1 - \Delta_{\mathrm{sec},i}]$, where $\tilde{R}_i$ is the expected ratio from prompt D mesons (those produced at the PV), and $\Delta_{\mathrm{sec},i}$ is the correction due to secondary decays. By measuring the fraction of secondary decays in RS candidates, $f_{\mathrm{sec},i}$, one can bound $\Delta_{\mathrm{sec},i}$ on both sides

$$f_{\mathrm{sec},i}\left[1 - \frac{R_{\max}(\hat{t}_i)}{R(\hat{t}_i)}\right] \le \Delta_{\mathrm{sec},i} \le f_{\mathrm{sec},i}\left[1 - \frac{R_{\min}(\hat{t}_i)}{R(\hat{t}_i)}\right]. \quad (2)$$

The function $R(t)$ is defined in Eq. (1), and $\hat{t}_i$ is the average decay time in decay-time bin i. The expressions $R_{\min}(\hat{t}_i)$ and $R_{\max}(\hat{t}_i)$ give the minimum and maximum of Eq. (1) in the decay-time range $[0, \hat{t}_i]$. To determine the secondary fractions $f_{\mathrm{sec},i}$ a discriminating variable based on the D^0 impact parameter relative to the PV is fitted with both a prompt and secondary component: the PDF describing the former is determined from signal candidates with decay times smaller than 0.8τ, and the PDF describing the latter is found from a subsample of candidates that are compatible with the decay chain $B \to D^{*\pm}\mu X$. From these fits the secondary fraction is seen to increase monotonically with decay time from $(1.6 \pm 1.1)\%$ to $(6.9 \pm 0.6)\%$.

The efficiency to trigger, reconstruct, and select a $D^0 \to K^+\pi^-\pi^+\pi^-$ candidate depends on its location in the five-dimensional phase space of the decay. Since there are differences in the amplitude structure between WS and RS decays, the measured WS/RS ratio can be biased. The efficiency is therefore determined in five-dimensional phase space bins using simulated data. In each decay-time bin this is used to correct the WS/RS yields taking into account the observed five-dimensional event distribution. The resulting multiplicative correction factors to the
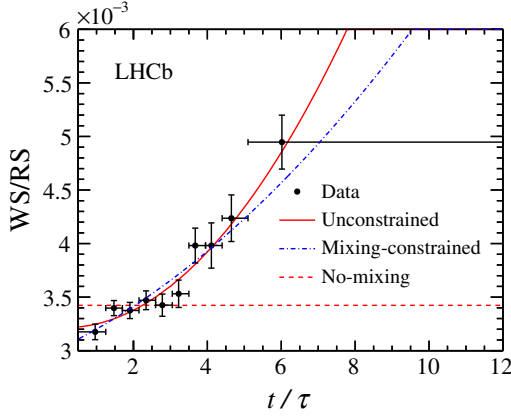
FIG. 2.   Decay-time evolution of the background-subtracted and efficiency corrected WS/RS ratio (points) with the results of the unconstrained (solid line), mixing-constrained (dashed-dotted line), and no-mixing (dashed line) fits superimposed. The bin centers are set to the decay time where $R(t)$ is equal to the bin integrated ratio $\tilde{R}$ from the unconstrained fit.

WS/RS ratio ϵ_i differ from unity by less than a few percent, and increase (decrease) the ratio at low (high) decay times.

The background-subtracted and efficiency corrected WS/RS ratio measured in the ith decay-time bin is given by $\tilde{r}_i \equiv r_i \epsilon_i - \Delta_{\mathrm{ID},i} - \Delta_{K_S^0}$, where r_i is the WS/RS ratio estimated from the Δm fit. The parameters of interest are determined by minimizing the χ^2 function

$$\chi^2(\tilde{\mathbf{r}}, C|\boldsymbol{\theta}) = \sum_{i,j=1}^{10} [\tilde{r}_i - \tilde{R}_i(\boldsymbol{\theta})[1 - \Delta_{\mathrm{sec},i}]]$$
$$\times [C^{-1}]_{ij}[\tilde{r}_j - \tilde{R}_j(\boldsymbol{\theta})[1 - \Delta_{\mathrm{sec},j}]]$$
$$+ \chi^2_{\mathrm{sec}}(\boldsymbol{\theta})[+\chi^2_{x,y}(\boldsymbol{\theta})], \qquad (3)$$

where C is the full covariance matrix of the measurements, including statistical and systematic uncertainties. Here, $\tilde{R}_i(\boldsymbol{\theta})$ gives the theoretical ratio of WS to RS decay rates [Eq. (1)], integrated over the ith decay-time bin, which depends on the fit parameter vector $\boldsymbol{\theta} = \{r_D^{K3\pi},$ $R_D^{K3\pi}y'_{K3\pi}, \frac{1}{4}(x^2 + y^2)\}$. Also included in the determination

of $\tilde{R}_i(\boldsymbol{\theta})$ is the decay-time acceptance, which is found from the RS candidates assuming that their decay-time dependence is exponential. The parameters $\Delta_{\mathrm{sec},i}$ are free to float in the fit with a Gaussian constraint χ^2_{sec}. The mean and width of the Gaussian constraints are defined to be the midpoint and half the difference between the limits in Eq. (2), respectively, which are dynamically updated during the fit. The parameters $f_{\mathrm{sec},i}$ (which are required to calculate these limits) are also Gaussian constrained to their measured values. An alternate fit is also performed where the mixing parameters x and y are constrained to world average values [4] $x = (0.371 \pm 0.158) \times 10^{-2}$ and $y = (0.656 \pm 0.080) \times 10^{-2}$ with a correlation coefficient of -0.361. In this case an additional term $\chi^2_{x,y}$ is included in the fit and $\boldsymbol{\theta} = \{r_D^{K3\pi}, R_D^{K3\pi}y'_{K3\pi}, x, y\}$. The two fit configurations are referred to as "unconstrained" and "mixing constrained".

Figure 2 shows the decay-time dependent fits to the WS/ RS ratio for the unconstrained, mixing-constrained, and no-mixing fit configurations; the latter has the fit parameters $R_D^{K3\pi} \cdot y'_{K3\pi}$ and $\frac{1}{4}(x^2 + y^2)$ fixed to zero. The numerical results of the unconstrained and mixing-constrained fit configurations are presented in Table I. The values of $R_D^{K3\pi}y'_{K3\pi}$ and $\frac{1}{4}(x^2 + y^2)$ from the unconstrained fit are both compatible with zero at less than 3 standard deviations, but due to the large correlation between these parameters, the hypothesis that both are zero can be rejected with much higher significance. Using Wilks' theorem [29] the no-mixing hypothesis is excluded at a significance level of 8.2 standard deviations. The value of $\frac{1}{4}(x^2 + y^2)$ determined using the world average values of x and y is compatible with the unconstrained fit result at 1.8 standard deviations. The results of the mixing-constrained fit show that the uncertainties on the parameters $r_D^{K3\pi}$ and $R_D^{K3\pi}y'_{K3\pi}$ are reduced by 41% and 61%, respectively, in comparison with the unconstrained fit. Using the mixing-constrained fit, it is possible to identify a line of solutions in the $(R_D^{K3\pi}, \delta_D^{K3\pi})$ plane. The two-dimensional contours containing 68.3%, 95.4%, and 99.7% confidence regions are shown in Fig. 3. The only other constraints on

TABLE I.   Results of the decay-time dependent fits to the WS/RS ratio for the unconstrained and mixing-constrained fit configurations. The results include all systematic uncertainties. The number of degrees of freedom is abbreviated as ndf

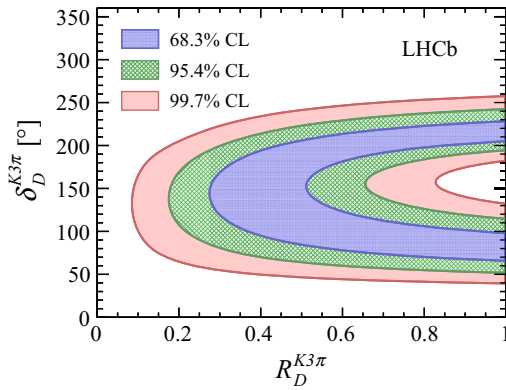| Fit Type χ^2/ndf (p value)	Parameter	Fit result	$r_D^{K3\pi}$	Correlation coefficient $R_D^{K3\pi}y'_{K3\pi}$	$\frac{1}{4}(x^2 + y^2)$	
Unconstrained 7.8/7(0.35)	$r_D^{K3\pi}$ $R_D^{K3\pi}y'_{K3\pi}$ $\frac{1}{4}(x^2 + y^2)$	$(5.67 \pm 0.12) \times 10^{-2}$ $(0.3 \pm 1.8) \times 10^{-3}$ $(4.8 \pm 1.8) \times 10^{-5}$	1	0.91 1	0.80 0.94 1	
			$r_D^{K3\pi}$	$R_D^{K3\pi}y'_{K3\pi}$	x	y
Mixing constrained 11.2/8(0.19)	$r_D^{K3\pi}$ $R_D^{K3\pi}y'_{K3\pi}$ x y	$(5.50 \pm 0.07) \times 10^{-2}$ $(-3.0 \pm 0.7) \times 10^{-3}$ $(4.1 \pm 1.7) \times 10^{-3}$ $(6.7 \pm 0.8) \times 10^{-3}$	1	0.83 1	0.17 0.34 1	0.10 0.20 -0.40 1

FIG. 3.   Confidence-level (C.L.) regions in the $R_D^{K3\pi} - \delta_D^{K3\pi}$ plane taken from the mixing-constrained fit.

$(R_D^{K3\pi}, \delta_D^{K3\pi})$ are based on CLEO-c data [30]. A combination would require a combined fit sharing the input on x and y. A combination made ignoring this complication shows that the input from mixing results in reductions in uncertainties on $R_D^{K3\pi}$ and $\delta_D^{K3\pi}$ by approximately 50% when compared to the CLEO-c values.

To evaluate the impact of systematic uncertainties included in the result, the fits are repeated with the systematic uncertainties on the WS/RS ratio set to zero. In the unconstrained fit the uncertainties in $r_D^{K3\pi}$, $R_D^{K3\pi} y'_{K3\pi}$, and $\frac{1}{4}(x^2 + y^2)$ are reduced by 11%, 9%, and 11%, respectively. In the mixing-constrained fit the uncertainties in $r_D^{K3\pi}$ and $R_D^{K3\pi} y'_{K3\pi}$ are reduced by 15% and 9%, respectively.

Using the results presented in Table I the decay-time integrated WS/RS ratio $R_{WS}^{K3\pi} = (r_D^{K3\pi})^2 - r_D^{K3\pi} R_D^{K3\pi} y'_{K3\pi} + \frac{1}{2}(x^2 + y^2)$ is calculated to be $(3.29 \pm 0.08) \times 10^{-3}$ for the unconstrained result, and $(3.22 \pm 0.05) \times 10^{-3}$ for the mixing-constrained result. This is consistent with the existing measurement from Belle [8], and has smaller uncertainties. Using the RS branching fraction $\mathcal{B}(D^0 \to K^-\pi^+\pi^-\pi^+) = (8.07 \pm 0.23) \times 10^{-2}$ [26], the WS branching fraction $\mathcal{B}(D^0 \to K^+\pi^-\pi^+\pi^-)$ is determined to be $(2.66 \pm 0.06 \pm 0.08) \times 10^{-4}$ using the unconstrained result, and $(2.60 \pm 0.04 \pm 0.07) \times 10^{-4}$ using the mixing-constrained result. Here, the first uncertainty is propagated from $R_{WS}^{K3\pi}$ and includes systematic effects, and the second is from the knowledge of $\mathcal{B}(D^0 \to K^-\pi^+\pi^-\pi^+)$.

In conclusion, the decay-time dependence of the ratio of $D^0 \to K^+\pi^-\pi^+\pi^-$ to $D^0 \to K^-\pi^+\pi^-\pi^+$ decay rates is observed, and the no-mixing hypothesis is excluded at a significance level of 8.2 standard deviations. The world's most precise measurements of $r_D^{K3\pi}$ and $R_{WS}^{K3\pi}$ are presented, and a unique constraint on $R_D^{K3\pi} y'_{K3\pi}$ is given, which will increase sensitivity to the CP-violating phase γ in $B^+ \to DK^+$, $D \to K^-\pi^+\pi^-\pi^+$ decays.

[1] B. Aubert *et al.* (*BABAR* Collaboration), Evidence for $D^0 - \bar{D}^0$ Mixing Phys. Rev. Lett. **98**, 211802 (2007).

[2] M. Staric *et al.* (Belle Collaboration), Evidence for $D^0 - \bar{D}^0$ Mixing, Phys. Rev. Lett. **98**, 211803 (2007).

[3] T. Aaltonen *et al.* (CDF Collaboration), Evidence for $D^0 - \bar{D}^0$ Mixing using the CDF II Detector, Phys. Rev. Lett. **100**, 121802 (2008).

[4] Y. Amhis *et al.* (Heavy Flavor Averaging Group), Averages of *b*-hadron, *c*-hadron, and τ-lepton properties as of summer 2014, arXiv:1412.7515. This Letter uses the CP violation allowed averages from the July 2015 update, which can be found at http://www.slac.stanford.edu/xorg/hfag/charm/CHARM15/results_mix_cpv.html.

[5] R. Aaij *et al.* (LHCb Collaboration), Observation of $D^0 - \bar{D}^0$ Oscillations, Phys. Rev. Lett.**110**, 101802 (2013).

[6] T. A. Aaltonen *et al.* (CDF Collaboration), Observation of $D^0 - \bar{D}^0$ Mixing using the CDF II Detector, Phys. Rev. Lett. **111**, 231802 (2013).

[7] B. R. Ko *et al.* (Belle Collaboration), Observation of $D^0 - \bar{D}^0$ Mixing in e^+e^- Collisions, Phys. Rev. Lett. **112**, 111801 (2014); **112**, 139903(A) (2014).

[8] E. White *et al.* (Belle Collaboration), Measurement of the wrong-sign decay $D^0 \to K^+\pi^-\pi^+\pi^-$, Phys. Rev. D **88**, 051101 (2013).

[9] M. G. Wilson *et al.* (*BABAR* Collaboration), Search for $D^0 - \bar{D}^0$ mixing in the decays $D^0 \to K^+\pi^-\pi^+\pi^-$, in Proceedings of the 33rd International Conference on High Energy Physics (ICHEP '06), Moscow, Russia, 26 July–2 August 2006, 2007.

[10] M. Gronau and D. Wyler, On determining a weak phase from CP asymmetries in charged B decays, Phys. Lett. B **265**, 172 (1991).

[11] M. Gronau and D. London, How to determine all the angles of the unitarity triangle from $B_d \to DK_s$ and $B_s^0 \to D\phi$, Phys. Lett. B **253**, 483 (1991).

[12] D. Atwood, I. Dunietz, and A. Soni, Enhanced CP Violation with $B \to KD^0(\bar{D}^0)$ Modes and Extraction of the Cabibbo-Kobayashi-Maskawa Angle γ, Phys. Rev. Lett. **78**, 3257 (1997).

[13] A. Giri, Y. Grossman, A. Soffer, and J. Zupan, Determining γ using $B^\pm \to DK^\pm$ with multibody D decays, Phys. Rev. D **68**, 054018 (2003).

[14] J. Rademacher and G. Wilkinson, Determining the unitarity triangle gamma with a four-body amplitude analysis of $B^+ \to (K^+K^-\pi^+\pi^-)_D K^\pm$ decays, Phys. Lett. B **647**, 400 (2007).

[15] S. Harnew and J. Rademacher, Charm mixing as input for model-independent determinations of the CKM phase γ, Phys. Lett. B **728**, 296 (2014).

[16] S. Harnew and J. Rademacher, Model independent determination of the CKM phase γ using input from $D^0 - \bar{D}^0$ mixing, J. High Energy Phys. 03 (2015) 169.

[17] A. A. Alves Jr. et al. (LHCb Collaboration), The LHCb detector at the LHC, J. Instrum. **3**, S08005 (2008).

[18] R. Aaij et al. (LHCb Collaboration), LHCb detector performance, Int. J. Mod. Phys. A **30**, 1530022 (2015).

[19] T. Sjöstrand, S. Mrenna, and P. Skands, PYTHIA 6.4 physics and manual, J. High Energy Phys. 05 (2006) 026; T. Sjöstrand, S. Mrenna, and P. Skands, A brief introduction to PYTHIA 8.1, Comput. Phys. Commun. **178**, 852 (2008).

[20] I. Belyaev et al., Handling of the generation of primary events in Gauss, the LHCb simulation framework, J. Phys. Conf. Ser. **331**, 032047 (2011).

[21] J. Allison et al. (Geant4 Collaboration), Geant4 developments and applications, IEEE Trans. Nucl. Sci. **53**, 270 (2006).

[22] M. Clemencic, G. Corti, S. Easo, C. R. Jones, S. Miglioranzi, M. Pappagallo, and P. Robbe, The LHCb simulation application, Gauss: Design, evolution and experience, J. Phys. Conf. Ser. **331**, 032023 (2011).

[23] R. Aaij et al. (LHCb Collaboration), Measurement of the track reconstruction efficiency at LHCb, J. Instrum. **10**, P02007 (2015).

[24] R. Aaij et al. (LHCb Collaboration), Measurement of the $B_s^0 \to \phi\phi$ branching fraction and search for the decay $B^0 \to \phi\phi$, J. High Energy Phys. 10 (2015) 053.

[25] R. Aaij et al., The LHCb trigger and its performance in 2011, J. Instrum. **8**, P04022 (2013).

[26] K. A. Olive et al. (Particle Data Group), Review of particle physics, Chin. Phys. C **38**, 090001 (2014). See also the 2015 update.

[27] N. L. Johnson, Systems of frequency curves generated by methods of translation, Biometrika **36**, 149 (1949).

[28] R. Aaij et al. (LHCb Collaboration), Measurement of $D^0 - \bar{D}^0$ Mixing Parameters and Search for CP Violation using $D^0 \to K^+\pi^-$ Decays, Phys. Rev. Lett. **111**, 251801 (2013).

[29] S. S. Wilks, The large-sample distribution of the likelihood ratio for testing composite hypotheses, Ann. Math. Stat. **9**, 60 (1938).

[30] J. Libby et al., New determination of the $D^0 \to K^-\pi^+\pi^0$ and $D^0 \to K^-\pi^+\pi^+\pi^-$ coherence factors and average strong-phase differences, Phys. Lett. B **731**, 197 (2014).

R. Aaij,[39] C. Abellán Beteta,[41] B. Adeva,[38] M. Adinolfi,[47] A. Affolder,[53] Z. Ajaltouni,[5] S. Akar,[6] J. Albrecht,[10] F. Alessio,[39] M. Alexander,[52] S. Ali,[42] G. Alkhazov,[31] P. Alvarez Cartelle,[54] A. A. Alves Jr.,[58] S. Amato,[2] S. Amerio,[23] Y. Amhis,[7] L. An,[3,40] L. Anderlini,[18] G. Andreassi,[40] M. Andreotti,[17,a] J. E. Andrews,[59] R. B. Appleby,[55] O. Aquines Gutierrez,[11] F. Archilli,[39] P. d'Argent,[12] A. Artamonov,[36] M. Artuso,[60] E. Aslanides,[6] G. Auriemma,[26,b] M. Baalouch,[5] S. Bachmann,[12] J. J. Back,[49] A. Badalov,[37] C. Baesso,[61] W. Baldini,[17,39] R. J. Barlow,[55] C. Barschel,[39] S. Barsuk,[7] W. Barter,[39] V. Batozskaya,[29] V. Battista,[40] A. Bay,[40] L. Beaucourt,[4] J. Beddow,[52] F. Bedeschi,[24] I. Bediaga,[1] L. J. Bel,[42] V. Bellee,[40] N. Belloli,[21,c] I. Belyaev,[32] E. Ben-Haim,[8] G. Bencivenni,[19] S. Benson,[39] J. Benton,[47] A. Berezhnoy,[33] R. Bernet,[41] A. Bertolin,[23] F. Betti,[15] M.-O. Bettler,[39] M. van Beuzekom,[42] S. Bifani,[46] P. Billoir,[8] T. Bird,[55] A. Birnkraut,[10] A. Bizzeti,[18,d] T. Blake,[49] F. Blanc,[40] J. Blouw,[11] S. Blusk,[60] V. Bocci,[26] A. Bondar,[35] N. Bondar,[31,39] W. Bonivento,[16] A. Borgheresi,[21,c] S. Borghi,[55] M. Borisyak,[66] M. Borsato,[38] T. J. V. Bowcock,[53] E. Bowen,[41] C. Bozzi,[17,39] S. Braun,[12] M. Britsch,[12] T. Britton,[60] J. Brodzicka,[55] N. H. Brook,[47] E. Buchanan,[47] C. Burr,[55] A. Bursche,[2] J. Buytaert,[39] S. Cadeddu,[16] R. Calabrese,[17,a] M. Calvi,[21,c] M. Calvo Gomez,[37,e] P. Campana,[19] D. Campora Perez,[39] L. Capriotti,[55] A. Carbone,[15,f] G. Carboni,[25,g] R. Cardinale,[20,h] A. Cardini,[16] P. Carniti,[21,c] L. Carson,[51] K. Carvalho Akiba,[2] G. Casse,[53] L. Cassina,[21,c] L. Castillo Garcia,[40] M. Cattaneo,[39] Ch. Cauet,[10] G. Cavallero,[20] R. Cenci,[24,i] M. Charles,[8] Ph. Charpentier,[39] M. Chefdeville,[4] S. Chen,[55] S.-F. Cheung,[56] N. Chiapolini,[41] M. Chrzaszcz,[41,27] X. Cid Vidal,[39] G. Ciezarek,[42] P. E. L. Clarke,[51] M. Clemencic,[39] H. V. Cliff,[48] J. Closier,[39] V. Coco,[39] J. Cogan,[6] E. Cogneras,[5] V. Cogoni,[16,j] L. Cojocariu,[30] G. Collazuol,[23,k] P. Collins,[39] A. Comerma-Montells,[12] A. Contu,[39] A. Cook,[47] M. Coombes,[47] S. Coquereau,[8] G. Corti,[39] M. Corvo,[17,a] B. Couturier,[39] G. A. Cowan,[51] D. C. Craik,[51] A. Crocombe,[49] M. Cruz Torres,[61] S. Cunliffe,[54] R. Currie,[54] C. D'Ambrosio,[39] E. Dall'Occo,[42] J. Dalseno,[47] P. N. Y. David,[42] A. Davis,[58] O. De Aguiar Francisco,[2] K. De Bruyn,[6] S. De Capua,[55] M. De Cian,[12] J. M. De Miranda,[1] L. De Paula,[2] P. De Simone,[19]

C.-T. Dean,[52] D. Decamp,[4] M. Deckenhoff,[10] L. Del Buono,[8] N. Déléage,[4] M. Demmer,[10] D. Derkach,[66] O. Deschamps,[5] F. Dettori,[39] B. Dey,[22] A. Di Canto,[39] F. Di Ruscio,[25] H. Dijkstra,[39] S. Donleavy,[53] F. Dordei,[39] M. Dorigo,[40] A. Dosil Suárez,[38] A. Dovbnya,[44] K. Dreimanis,[53] L. Dufour,[42] G. Dujany,[55] K. Dungs,[39] P. Durante,[39] R. Dzhelyadin,[36] A. Dziurda,[27] A. Dzyuba,[31] S. Easo,[50,39] U. Egede,[54] V. Egorychev,[32] S. Eidelman,[35] S. Eisenhardt,[51] U. Eitschberger,[10] R. Ekelhof,[10] L. Eklund,[52] I. El Rifai,[5] Ch. Elsasser,[41] S. Ely,[60] S. Esen,[12] H. M. Evans,[48] T. Evans,[56] A. Falabella,[15] C. Färber,[39] N. Farley,[46] S. Farry,[53] R. Fay,[53] D. Fazzini,[21,c] D. Ferguson,[51] V. Fernandez Albor,[38] F. Ferrari,[15] F. Ferreira Rodrigues,[1] M. Ferro-Luzzi,[39] S. Filippov,[34] M. Fiore,[17,39,a] M. Fiorini,[17,a] M. Firlej,[28] C. Fitzpatrick,[40] T. Fiutowski,[28] F. Fleuret,[7,l] K. Fohl,[39] P. Fol,[54] M. Fontana,[16] F. Fontanelli,[20,h] D. C. Forshaw,[60] R. Forty,[39] M. Frank,[39] C. Frei,[39] M. Frosini,[18] J. Fu,[22] E. Furfaro,[25,g] A. Gallas Torreira,[38] D. Galli,[15,f] S. Gallorini,[23] S. Gambetta,[51] M. Gandelman,[2] P. Gandini,[56] Y. Gao,[3] J. García Pardiñas,[38] J. Garra Tico,[48] L. Garrido,[37] D. Gascon,[37] C. Gaspar,[39] L. Gavardi,[10] G. Gazzoni,[5] D. Gerick,[12] E. Gersabeck,[12] M. Gersabeck,[55] T. Gershon,[49] Ph. Ghez,[4] S. Gianì,[40] V. Gibson,[48] O. G. Girard,[40] L. Giubega,[30] V. V. Gligorov,[39] C. Göbel,[61] D. Golubkov,[32] A. Golutvin,[54,39] A. Gomes,[1,m] C. Gotti,[21,c] M. Grabalosa Gándara,[5] R. Graciani Diaz,[37] L. A. Granado Cardoso,[39] E. Graugés,[37] E. Graverini,[41] G. Graziani,[18] A. Grecu,[30] P. Griffith,[46] L. Grillo,[12] O. Grünberg,[64] B. Gui,[60] E. Gushchin,[34] Yu. Guz,[36,39] T. Gys,[39] T. Hadavizadeh,[56] C. Hadjivasiliou,[60] G. Haefeli,[40] C. Haen,[39] S. C. Haines,[48] S. Hall,[54] B. Hamilton,[59] X. Han,[12] S. Hansmann-Menzemer,[12] N. Harnew,[56] S. T. Harnew,[47] J. Harrison,[55] J. He,[39] T. Head,[40] V. Heijne,[42] A. Heister,[9] K. Hennessy,[53] P. Henrard,[5] L. Henry,[8] J. A. Hernando Morata,[38] E. van Herwijnen,[39] M. Heß,[64] A. Hicheur,[2] D. Hill,[56] M. Hoballah,[5] C. Hombach,[55] L. Hongming,[40] W. Hulsbergen,[42] T. Humair,[54] M. Hushchyn,[66] N. Hussain,[56] D. Hutchcroft,[53] D. Hynds,[52] M. Idzik,[28] P. Ilten,[57] R. Jacobsson,[39] A. Jaeger,[12] J. Jalocha,[56] E. Jans,[42] A. Jawahery,[59] M. John,[56] D. Johnson,[39] C. R. Jones,[48] C. Joram,[39] B. Jost,[39] N. Jurik,[60] S. Kandybei,[44] W. Kanso,[6] M. Karacson,[39] T. M. Karbach,[39] S. Karodia,[52] M. Kecke,[12] M. Kelsey,[60] I. R. Kenyon,[46] M. Kenzie,[39] T. Ketel,[43] E. Khairullin,[66] B. Khanji,[21,39,c] C. Khurewathanakul,[40] T. Kirn,[9] S. Klaver,[55] K. Klimaszewski,[29] O. Kochebina,[7] M. Kolpin,[12] I. Komarov,[40] R. F. Koopman,[43] P. Koppenburg,[42,39] M. Kozeiha,[5] L. Kravchuk,[34] K. Kreplin,[12] M. Kreps,[49] P. Krokovny,[35] F. Kruse,[10] W. Krzemien,[29] W. Kucewicz,[27,n] M. Kucharczyk,[27] V. Kudryavtsev,[35] A. K. Kuonen,[40] K. Kurek,[29] T. Kvaratskheliya,[32] D. Lacarrere,[39] G. Lafferty,[55,39] A. Lai,[16] D. Lambert,[51] G. Lanfranchi,[19] C. Langenbruch,[49] B. Langhans,[39] T. Latham,[49] C. Lazzeroni,[46] R. Le Gac,[6] J. van Leerdam,[42] J.-P. Lees,[4] R. Lefèvre,[5] A. Leflat,[33,39] J. Lefrançois,[7] E. Lemos Cid,[38] O. Leroy,[6] T. Lesiak,[27] B. Leverington,[12] Y. Li,[7] T. Likhomanenko,[66,65] M. Liles,[53] R. Lindner,[39] C. Linn,[39] F. Lionetto,[41] B. Liu,[16] X. Liu,[3] D. Loh,[49] I. Longstaff,[52] J. H. Lopes,[2] D. Lucchesi,[23,k] M. Lucio Martinez,[38] H. Luo,[51] A. Lupato,[23] E. Luppi,[17,a] O. Lupton,[56] N. Lusardi,[22] A. Lusiani,[24] F. Machefert,[7] F. Maciuc,[30] O. Maev,[31] K. Maguire,[55] S. Malde,[56] A. Malinin,[65] G. Manca,[7] G. Mancinelli,[6] P. Manning,[60] A. Mapelli,[39] J. Maratas,[5] J. F. Marchand,[4] U. Marconi,[15] C. Marin Benito,[37] P. Marino,[24,39,i] J. Marks,[12] G. Martellotti,[26] M. Martin,[6] M. Martinelli,[40] D. Martinez Santos,[38] F. Martinez Vidal,[67] D. Martins Tostes,[2] L. M. Massacrier,[7] A. Massafferri,[1] R. Matev,[39] A. Mathad,[49] Z. Mathe,[39] C. Matteuzzi,[21] A. Mauri,[41] B. Maurin,[40] A. Mazurov,[46] M. McCann,[54] J. McCarthy,[46] A. McNab,[55] R. McNulty,[13] B. Meadows,[58] F. Meier,[10] M. Meissner,[12] D. Melnychuk,[29] M. Merk,[42] A Merli,[22,o] E Michielin,[23] D. A. Milanes,[63] M.-N. Minard,[4] D. S. Mitzel,[12] J. Molina Rodriguez,[61] I. A. Monroy,[63] S. Monteil,[5] M. Morandin,[23] P. Morawski,[28] A. Mordà,[6] M. J. Morello,[24,i] J. Moron,[28] A. B. Morris,[51] R. Mountain,[60] F. Muheim,[51] D. Müller,[55] J. Müller,[10] K. Müller,[41] V. Müller,[10] M. Mussini,[15] B. Muster,[40] P. Naik,[47] T. Nakada,[40] R. Nandakumar,[50] A. Nandi,[56] I. Nasteva,[2] M. Needham,[51] N. Neri,[22] S. Neubert,[12] N. Neufeld,[39] M. Neuner,[12] A. D. Nguyen,[40] C. Nguyen-Mau,[40,p] V. Niess,[5] S. Nieswand,[9] R. Niet,[10] N. Nikitin,[33] T. Nikodem,[12] A. Novoselov,[36] D. P. O'Hanlon,[49] A. Oblakowska-Mucha,[28] V. Obraztsov,[36] S. Ogilvy,[52] O. Okhrimenko,[45] R. Oldeman,[16,48,j] C. J. G. Onderwater,[68] B. Osorio Rodrigues,[1] J. M. Otalora Goicochea,[2] A. Otto,[39] P. Owen,[54] A. Oyanguren,[67] A. Palano,[14,q] F. Palombo,[22,o] M. Palutan,[19] J. Panman,[39] A. Papanestis,[50] M. Pappagallo,[52] L. L. Pappalardo,[17,a] C. Pappenheimer,[58] W. Parker,[59] C. Parkes,[55] G. Passaleva,[18] G. D. Patel,[53] M. Patel,[54] C. Patrignani,[20,h] A. Pearce,[55,50] A. Pellegrino,[42] G. Penso,[26,r] M. Pepe Altarelli,[39] S. Perazzini,[15,f] P. Perret,[5] L. Pescatore,[46] K. Petridis,[47] A. Petrolini,[20,h] M. Petruzzo,[22] E. Picatoste Olloqui,[37] B. Pietrzyk,[4] M. Pikies,[27] D. Pinci,[26] A. Pistone,[20] A. Piucci,[12] S. Playfer,[51] M. Plo Casasus,[38] T. Poikela,[39] F. Polci,[8] A. Poluektov,[49,35] I. Polyakov,[32] E. Polycarpo,[2] A. Popov,[36] D. Popov,[11,39] B. Popovici,[30] C. Potterat,[2] E. Price,[47] J. D. Price,[53] J. Prisciandaro,[38] A. Pritchard,[53] C. Prouve,[47] V. Pugatch,[45] A. Puig Navarro,[40] G. Punzi,[24,s] W. Qian,[56] R. Quagliani,[7,47] B. Rachwal,[27] J. H. Rademacker,[47] M. Rama,[24] M. Ramos Pernas,[38] M. S. Rangel,[2] I. Raniuk,[44] G. Raven,[43] F. Redi,[54] S. Reichert,[55] A. C. dos Reis,[1] V. Renaudin,[7] S. Ricciardi,[50] S. Richards,[47] M. Rihl,[39] K. Rinnert,[53,39] V. Rives Molina,[37] P. Robbe,[7,39] A. B. Rodrigues,[1] E. Rodrigues,[55]

J. A. Rodriguez Lopez,[63] P. Rodriguez Perez,[55] A. Rogozhnikov,[66] S. Roiser,[39] V. Romanovsky,[36] A. Romero Vidal,[38]
J. W. Ronayne,[13] M. Rotondo,[23] T. Ruf,[39] P. Ruiz Valls,[67] J. J. Saborido Silva,[38] N. Sagidova,[31] B. Saitta,[16,j]
V. Salustino Guimaraes,[2] C. Sanchez Mayordomo,[67] B. Sanmartin Sedes,[38] R. Santacesaria,[26] C. Santamarina Rios,[38]
M. Santimaria,[19] E. Santovetti,[25,g] A. Sarti,[19,r] C. Satriano,[26,b] A. Satta,[25] D. M. Saunders,[47] D. Savrina,[32,33] S. Schael,[9]
M. Schiller,[39] H. Schindler,[39] M. Schlupp,[10] M. Schmelling,[11] T. Schmelzer,[10] B. Schmidt,[39] O. Schneider,[40] A. Schopper,[39]
M. Schubiger,[40] M.-H. Schune,[7] R. Schwemmer,[39] B. Sciascia,[19] A. Sciubba,[26,r] A. Semennikov,[32] A. Sergi,[46] N. Serra,[41]
J. Serrano,[6] L. Sestini,[23] P. Seyfert,[21] M. Shapkin,[36] I. Shapoval,[17,44,a] Y. Shcheglov,[31] T. Shears,[53] L. Shekhtman,[35]
V. Shevchenko,[65] A. Shires,[10] B. G. Siddi,[17] R. Silva Coutinho,[41] L. Silva de Oliveira,[2] G. Simi,[23,s] M. Sirendi,[48]
N. Skidmore,[47] T. Skwarnicki,[60] E. Smith,[54] I. T. Smith,[51] J. Smith,[48] M. Smith,[55] H. Snoek,[42] M. D. Sokoloff,[58,39]
F. J. P. Soler,[52] F. Soomro,[40] D. Souza,[47] B. Souza De Paula,[2] B. Spaan,[10] P. Spradlin,[52] S. Sridharan,[39] F. Stagni,[39]
M. Stahl,[12] S. Stahl,[39] S. Stefkova,[54] O. Steinkamp,[41] O. Stenyakin,[36] S. Stevenson,[56] S. Stoica,[30] S. Stone,[60] B. Storaci,[41]
S. Stracka,[24,i] M. Straticiuc,[30] U. Straumann,[41] L. Sun,[58] W. Sutcliffe,[54] K. Swientek,[28] S. Swientek,[10] V. Syropoulos,[43]
M. Szczekowski,[29] T. Szumlak,[28] S. T'Jampens,[4] A. Tayduganov,[6] T. Tekampe,[10] G. Tellarini,[17,a] F. Teubert,[39] C. Thomas,[56]
E. Thomas,[39] J. van Tilburg,[42] V. Tisserand,[4] M. Tobin,[40] J. Todd,[58] S. Tolk,[43] L. Tomassetti,[17,a] D. Tonelli,[39]
S. Topp-Joergensen,[56] E. Tournefier,[4] S. Tourneur,[40] K. Trabelsi,[40] M. Traill,[52] M. T. Tran,[40] M. Tresch,[41] A. Trisovic,[39]
A. Tsaregorodtsev,[6] P. Tsopelas,[42] N. Tuning,[42,39] A. Ukleja,[29] A. Ustyuzhanin,[66,65] U. Uwer,[12] C. Vacca,[16,39,j] V. Vagnoni,[15]
G. Valenti,[15] A. Vallier,[7] R. Vazquez Gomez,[19] P. Vazquez Regueiro,[38] C. Vázquez Sierra,[38] S. Vecchi,[17] M. van Veghel,[43]
J. J. Velthuis,[47] M. Veltri,[18,t] G. Veneziano,[40] M. Vesterinen,[12] B. Viaud,[7] D. Vieira,[2] M. Vieites Diaz,[38]
X. Vilasis-Cardona,[37,e] V. Volkov,[33] A. Vollhardt,[41] D. Voong,[47] A. Vorobyev,[31] V. Vorobyev,[35] C. Voß,[64] J. A. de Vries,[42]
R. Waldi,[64] C. Wallace,[49] R. Wallace,[13] J. Walsh,[24] J. Wang,[60] D. R. Ward,[48] N. K. Watson,[46] D. Websdale,[54] A. Weiden,[41]
M. Whitehead,[39] J. Wicht,[49] G. Wilkinson,[56,39] M. Wilkinson,[60] M. Williams,[39] M. P. Williams,[46] M. Williams,[57]
T. Williams,[46] F. F. Wilson,[50] J. Wimberley,[59] J. Wishahi,[10] W. Wislicki,[29] M. Witek,[27] G. Wormser,[7] S. A. Wotton,[48]
K. Wraight,[52] S. Wright,[48] K. Wyllie,[39] Y. Xie,[62] Z. Xu,[40] Z. Yang,[3] H. Yin,[62] J. Yu,[62] X. Yuan,[35] O. Yushchenko,[36]
M. Zangoli,[15] M. Zavertyaev,[11,u] L. Zhang,[3] Y. Zhang,[3] A. Zhelezov,[12] A. Zhokhov,[32]
L. Zhong,[3] V. Zhukov,[9] and S. Zucchelli[15]

(LHCb Collaboration)

[1]*Centro Brasileiro de Pesquisas Físicas (CBPF), Rio de Janeiro, Brazil*
[2]*Universidade Federal do Rio de Janeiro (UFRJ), Rio de Janeiro, Brazil*
[3]*Center for High Energy Physics, Tsinghua University, Beijing, China*
[4]*LAPP, Université Savoie Mont-Blanc, CNRS/IN2P3, Annecy-Le-Vieux, France*
[5]*Clermont Université, Université Blaise Pascal, CNRS/IN2P3, LPC, Clermont-Ferrand, France*
[6]*CPPM, Aix-Marseille Université, CNRS/IN2P3, Marseille, France*
[7]*LAL, Université Paris-Sud, CNRS/IN2P3, Orsay, France*
[8]*LPNHE, Université Pierre et Marie Curie, Université Paris Diderot, CNRS/IN2P3, Paris, France*
[9]*I. Physikalisches Institut, RWTH Aachen University, Aachen, Germany*
[10]*Fakultät Physik, Technische Universität Dortmund, Dortmund, Germany*
[11]*Max-Planck-Institut für Kernphysik (MPIK), Heidelberg, Germany*
[12]*Physikalisches Institut, Ruprecht-Karls-Universität Heidelberg, Heidelberg, Germany*
[13]*School of Physics, University College Dublin, Dublin, Ireland*
[14]*Sezione INFN di Bari, Bari, Italy*
[15]*Sezione INFN di Bologna, Bologna, Italy*
[16]*Sezione INFN di Cagliari, Cagliari, Italy*
[17]*Sezione INFN di Ferrara, Ferrara, Italy*
[18]*Sezione INFN di Firenze, Firenze, Italy*
[19]*Laboratori Nazionali dell'INFN di Frascati, Frascati, Italy*
[20]*Sezione INFN di Genova, Genova, Italy*
[21]*Sezione INFN di Milano Bicocca, Milano, Italy*
[22]*Sezione INFN di Milano, Milano, Italy*
[23]*Sezione INFN di Padova, Padova, Italy*
[24]*Sezione INFN di Pisa, Pisa, Italy*
[25]*Sezione INFN di Roma Tor Vergata, Roma, Italy*
[26]*Sezione INFN di Roma La Sapienza, Roma, Italy*

[27]Henryk Niewodniczanski Institute of Nuclear Physics Polish Academy of Sciences, Kraków, Poland

[28]AGH - University of Science and Technology, Faculty of Physics and Applied Computer Science, Kraków, Poland

[29]National Center for Nuclear Research (NCBJ), Warsaw, Poland

[30]Horia Hulubei National Institute of Physics and Nuclear Engineering, Bucharest-Magurele, Romania

[31]Petersburg Nuclear Physics Institute (PNPI), Gatchina, Russia

[32]Institute of Theoretical and Experimental Physics (ITEP), Moscow, Russia

[33]Institute of Nuclear Physics, Moscow State University (SINP MSU), Moscow, Russia

[34]Institute for Nuclear Research of the Russian Academy of Sciences (INR RAN), Moscow, Russia

[35]Budker Institute of Nuclear Physics (SB RAS) and Novosibirsk State University, Novosibirsk, Russia

[36]Institute for High Energy Physics (IHEP), Protvino, Russia

[37]Universitat de Barcelona, Barcelona, Spain

[38]Universidad de Santiago de Compostela, Santiago de Compostela, Spain

[39]European Organization for Nuclear Research (CERN), Geneva, Switzerland

[40]Ecole Polytechnique Fédérale de Lausanne (EPFL), Lausanne, Switzerland

[41]Physik-Institut, Universität Zürich, Zürich, Switzerland

[42]Nikhef National Institute for Subatomic Physics, Amsterdam, The Netherlands

[43]Nikhef National Institute for Subatomic Physics and VU University Amsterdam, Amsterdam, The Netherlands

[44]NSC Kharkiv Institute of Physics and Technology (NSC KIPT), Kharkiv, Ukraine

[45]Institute for Nuclear Research of the National Academy of Sciences (KINR), Kyiv, Ukraine

[46]University of Birmingham, Birmingham, United Kingdom

[47]H. H. Wills Physics Laboratory, University of Bristol, Bristol, United Kingdom

[48]Cavendish Laboratory, University of Cambridge, Cambridge, United Kingdom

[49]Department of Physics, University of Warwick, Coventry, United Kingdom

[50]STFC Rutherford Appleton Laboratory, Didcot, United Kingdom

[51]School of Physics and Astronomy, University of Edinburgh, Edinburgh, United Kingdom

[52]School of Physics and Astronomy, University of Glasgow, Glasgow, United Kingdom

[53]Oliver Lodge Laboratory, University of Liverpool, Liverpool, United Kingdom

[54]Imperial College London, London, United Kingdom

[55]School of Physics and Astronomy, University of Manchester, Manchester, United Kingdom

[56]Department of Physics, University of Oxford, Oxford, United Kingdom

[57]Massachusetts Institute of Technology, Cambridge, Massachusetts, USA

[58]University of Cincinnati, Cincinnati, Ohio, USA

[59]University of Maryland, College Park, Maryland, USA

[60]Syracuse University, Syracuse, New York, USA

[61]Pontifícia Universidade Católica do Rio de Janeiro (PUC-Rio), Rio de Janeiro, Brazil
(associated with Universidade Federal do Rio de Janeiro (UFRJ), Rio de Janeiro, Brazil)

[62]Institute of Particle Physics, Central China Normal University, Wuhan, Hubei, China
(associated with Center for High Energy Physics, Tsinghua University, Beijing, China)

[63]Departamento de Fisica , Universidad Nacional de Colombia, Bogota, Colombia
(associated with LPNHE, Université Pierre et Marie Curie, Université Paris Diderot, CNRS/IN2P3, Paris, France)

[64]Institut für Physik, Universität Rostock, Rostock, Germany
(associated with Physikalisches Institut, Ruprecht-Karls-Universität Heidelberg, Heidelberg, Germany)

[65]National Research Centre Kurchatov Institute, Moscow, Russia
(associated with Institute of Theoretical and Experimental Physics (ITEP), Moscow, Russia)

[66]Yandex School of Data Analysis, Moscow, Russia
(associated with Institute of Theoretical and Experimental Physics (ITEP), Moscow, Russia)

[67]Instituto de Fisica Corpuscular (IFIC), Universitat de Valencia-CSIC, Valencia, Spain
(associated with Universitat de Barcelona, Barcelona, Spain)

[68]Van Swinderen Institute, University of Groningen, Groningen, The Netherlands
(associated with Nikhef National Institute for Subatomic Physics, Amsterdam, The Netherlands)

[a]Also at Università di Ferrara, Ferrara, Italy.

[b]Also at Università della Basilicata, Potenza, Italy.

[c]Also at Università di Milano Bicocca, Milano, Italy.

[d]Also at Università di Modena e Reggio Emilia, Modena, Italy.

[e]Also at LIFAELS, La Salle, Universitat Ramon Llull, Barcelona, Spain.

[f]Also at Università di Bologna, Bologna, Italy.

[g]Also at Università di Roma Tor Vergata, Roma, Italy.

[h]Also at Università di Genova, Genova, Italy.

[i]Also at Scuola Normale Superiore, Pisa, Italy.

[j]Also at Università di Cagliari, Cagliari, Italy.

[k]Also at Università di Padova, Padova, Italy.

[l]Also at Laboratoire Leprince-Ringuet, Palaiseau, France.

[m]Also at Universidade Federal do Triângulo Mineiro (UFTM), Uberaba-MG, Brazil.

[n]Also at AGH - University of Science and Technology, Faculty of Computer Science, Electronics and Telecommunications, Kraków, Poland.

[o]Also at Università degli Studi di Milano, Milano, Italy.

[p]Also at Hanoi University of Science, Hanoi, Viet Nam.

[q]Also at Università di Bari, Bari, Italy.

[r]Also at Università di Roma La Sapienza, Roma, Italy.

[s]Also at Università di Pisa, Pisa, Italy.

[t]Also at Università di Urbino, Urbino, Italy.

[u]Also at P.N. Lebedev Physical Institute, Russian Academy of Science (LPI RAS), Moscow, Russia.